Journal of Nuclear Medicine, published on April 23, 2021 as doi:10.2967/jnumed.120.246413

Metabolic Scar Assessment with ^{18}F-FDG -PET: Correlation to Ischemic VT Substrate and Successful Ablation Sites

Yousra Ghzally MD[1,2,3], Hasan Imanli MD[1,2], Mark Smith PhD[4], Jagat Mahat MBBS[1], Wengen Chen MD, PhD[1,3], Alejandro Jimenez MD[1,2], Mariem A. Sawan MD[1,2], Mohamed Aboel- Kassem F Abdelmegid MD, PhD[3], Hatem Abd el Rahman Helmy MD, PhD[3], Salwa Demitry MD, PhD[3], Vincent See MD[1,2], Stephen Shorofsky MD, PhD[1,2], Vasken Dilsizian MD[4], Timm Dickfeld MD, PhD[1,2]

Maryland Arrhythmia and Cardiology Imaging Group (MACIG)[1], Division of Cardiology, Department of Medicine[2], Assiut University, Egypt [3], University of Maryland, Department of Cardiovascular Medicine, Department of Diagnostic Radiology and Nuclear Medicine [4].

Word Count: 5029

Corresponding Author:

Timm Dickfeld, MD, PhD

Division of Cardiology

University of Maryland School of Medicine

22 S Greene St

Baltimore, MD,21201, USA

Email:tdickfel@som.umaryland.edu

Phone:(410)328-6056 Fax:(410)328-2062

First Author:

Yousra Ghzally, MD

yousraghzally@yahoo.com

Running Title: Metabolic VT Scar Assessment

Keywords: Functional imaging, ^{18}F-FDG- PET Imaging, Ventricular tachycardia substrate, VT channel/exit sites.

ABSTRACT

Background_ Functional/molecular imaging characteristics of ischemic ventricular tachycardia (VT) substrate are incompletely understood. Objective: Compare regional ^{18}F-FDG - PET tracer uptake with detailed electroanatomic maps (EAM) in a more extensive series of post-infarction VT patients to define metabolic properties of the VT substrate/successful ablation sites.

Methods_ 3D metabolic left ventricular (LV) reconstructions were created from perfusion-normalized ^{18}F-FDG images in consecutive patients undergoing VT ablation. Metabolic defects were defined as severe (<50% uptake) or moderate (50-70% uptake) referenced to the maximal 17-segmental uptake. Color-coded PET scars reconstructions were co-registered with corresponding high-resolution 3D EAM.

Results_ All 56 patients had ischemic cardiomyopathy (EF=29±12%). Severe PET defect (<50%) was larger than EAM voltage scar (<0.5mV) with 63.0±48.4cm² vs. 13.8±33.1cm² (p<0.001). Similarly, moderate/severe PET defect (≤70%) was larger than areas with abnormal voltage (≤1.5mV) measuring 105.1±67.2cm² vs. 56.2±62.6cm² (p<0.001). Analysis of bipolar voltage (n=23,389 mapping-points) showed decreased voltage among PET <50% (n=10,364; 0.5±0.3mV) to PET 50-70% (n=5,243; 1.5±0.9mV, p<0.01) with normal voltage among PET normal areas >70% (n=7,782, 3.2±1.3mV, p<0.001). Eighty-eight percent of VT channel/exit sites (n=44) were metabolically abnormal (PET <50%: 78%; PET 50-70%: 10%), while 12% (n=6) were in metabolically normal areas (PET>70%). Metabolic channels (n=26) existed in 45% (n=25) of patients with average length/width of 17.6±12.5mm/10.3±4.2mm. Metabolic channels were oriented apex/base (86%) predominantly, harboring VT channel/exit sites in 31%. Metabolic Rapid Transition Areas (RTA: >50% change of ^{18}F-FDG tracer uptake/15mm) were detected in 59% (n=33) co-localizing to VT channels/exit sites (15%) or its proximity (85%,

12.8±8.5mm). Metabolism-voltage mismatches (MVM) with PET<50%/voltage>1.5mV) were seen in 21% (n=12) harboring VT channel/exit sites in 41% of patients.

Conclusions_ Abnormal ^{18}F-FDG uptake categories can be detected using incremental 3D step-up reconstructions. They predicted decreasing bipolar voltages and VT channel/exit sites in ~90%. Additionally, functional imaging allowed detecting novel molecular tissue characteristics within the ischemic VT substrate such as metabolic channels, RTA, and MVM demonstrating intra-substrate heterogeneity and providing possible targets for imaging-guided ablation.

ABBREVIATIONS

EAM	Electro anatomical map
^{18}F-FDG - PET	Fluorodeoxyglucose Positron emission tomography
ICD	Implantable cardioverter-defibrillator
^{123}I-*m*IBG	Iodine-123-meta-iodobenzylguanidine
IHD	Ischemic heart disease.
LV	Left ventricle
LGE	Late Gadolinium enhancement
MRI	Magnetic resonance imaging
MVM	Metabolic voltage mismatch
RF	Radiofrequency
RTA	Rapid transition area
RV	Right ventricle
SPECT	Single-photon emission computed tomography
VT	Ventricular tachycardia

INTRODUCTION

Catheter ablation for ventricular tachycardia (VT) is an effective treatment option for patients with ischemic heart disease (IHD) and drug-refractory VT(*1*). Entrainment and activation mapping are the preferred VT mapping modalities but can only be performed in 10-30% of patients due to hemodynamic instability (*2*). Therefore surrogate strategies including pace mapping, ablation of diastolic potentials/late abnormal ventricular activation (*3*), or substrate-guided linear ablations (*4*) are commonly employed.

The current approaches using the gold standard of bipolar voltage mapping to define ischemic scar have a VT recurrence of up to 50% at 6-months (*5*). Bipolar voltage mapping has inherent limitations (e.g., assessing intramural scar, epicardial fat, limited spatial resolution, imperfect catheter contact). Therefore, structural imaging with late gadolinium enhancement cardiac magnetic resonance (LGE-CMR) or multi-detector computed tomography (MDCT) (*6-9*) has been used to assess anatomic changes (e.g., wall thickness/myocardial fibrosis). In contrast, functional imaging can successfully detect abnormal cellular function (e.g., metabolism/innervation) using ^{18}-fluorodeoxyglucose-positron emission tomography (^{18}F-FDG - PET) (*10,11*), and iodine-123-meta-iodobenzylguanidine (^{123}I-*m*IBG) scintigraphy (*12-14*).

^{18}F-FDG is recognized as one of the gold standards for the evaluation of ischemic substrate (*15,16*). It can provide direct information about the post-ischemic myocardial remodeling in IHD patients with VT and can safely be applied in implantable cardioverter-defibrillator (ICD) patients without metal artifacts affecting imaging quality. Prior small single-center studies suggested a good correlation between areas of decreased ^{18}F-FDG uptake and low bipolar voltage (*10,11,17-21*).

This study sought to compare in a larger cohort of ischemic VT patients detailed electroanatomic maps (EAM) with 3D ^{18}F-FDG -PET metabolic reconstructions to provide novel insights into the regional functional adaptation and heterogeneity of the post-ischemic VT substrate and identify possible imaging characteristics of VT channel/exit sites. PET thresholds used were based on prior work of our and other laboratories (*17,18,22*). Results may have differed with the utilization of other potential cut-offs.

METHODS

Study Population

The study was designed as a single-center retrospective feasibility study of 56 consecutive patients with ischemic cardiomyopathy scheduled for radiofrequency ablation for drug-refractory VT. Study protocols were approved by the University of Maryland Institutional Review Board.

Imaging

PET imaging was performed using a Philips Gemini system (Philips, Best, Netherlands) or a Siemens Biograph mCT PET/CT Scanner (Siemens Healthcare, Berlin, Germany).

Patients received an oral load of approximately 25-50 g of glucose following an overnight fast. 370-500 MBq of ^{18}F-FDG was injected approximately 1 hour later, and data were acquired over 25–30 minutes(*23*). Because the increase in plasma insulin levels after glucose loading may be attenuated in some patients, particularly those with diabetes mellitus, supplemental insulin was administered in these subsets of patients before the administration of ^{18}F-FDG, taking into account whether or not the patient was taking medications that may either antagonize or potentiate the effects of insulin, while monitoring their plasma glucose levels (*23*).

Regional myocardial blood flow was assessed by a pre-^{18}F-FDG -PET perfusion scan using either ^{82}Rubidium PET (n=50) or ^{201}Thallium (n=5) or ^{99m}Technetium sestamibi (n=1) single-photon emission tomography (SPECT).

PET perfusion images were obtained at rest using an 1850 MBq injection of 82-Rubidium (Rb) chloride. List-mode (i.e., time-stamped coincidence) data were acquired for 8 minutes after injection. An ungated perfusion image was reconstructed using data acquired 1.5–8 minutes after injection. A rotating Cesium-137-line source was used to perform a 3–4-minute attenuation correction scan for the ^{18}F-FDG and Rb data sets. Attenuation correction was not done for SPECT data (*24,25*). Myocardial perfusion images were reconstructed analogously to the ^{18}F-FDG -PET images. Both quantitative and qualitative assessments by nuclear cardiology experts were employed.

Electro-anatomic Mapping

High-density LV voltage maps were created with the CARTO 3® mapping system and a PentaRay catheter (Biosense Webster, Inc., Diamond Bar, CA, USA). Electro-anatomical data were collected with the catheter moving within the blood pool of the respective chamber with a <10mm filling threshold. It displays the endocardial surface created from usually >1000 individual mapping points color-coded based on the endocardial voltage. An endocardial bipolar voltage of >1.5mV recorded from the catheter is considered normal, representing healthy myocardium (purple color), while voltage <0.5mV is considered as a dense scar (red color). The voltages value of 0.5 to 1.5mV are considered border zones representing a mixture of scar and normal myocardium (yellow to blue color)(*4*).

3D Metabolic ^{18}F-FDG -PET Map Reconstruction and Integration with Voltage Maps

Short axis series of the PET DICOM files were loaded into the Amira Visual Imaging software (Visage Imaging, San Diego, USA). A left ventricle (LV) shell was created by manual tracing of the middle third of the LV in the Short axis series to accurately represent the peak tracer uptake in each LV segment. Partial right ventricle (RV) wall tracing was performed to aid the registration process (Figure 1A&1B). Quantitative radiotracer uptake analyses were performed using the PMOD Cardiac PET Modeling software Version 3.4 (PMOD Technologies, Zurich, Switzerland). For quantitative analysis, standard 17 segments myocardial segmentation was employed, and radiotracer uptake of each segment on both the perfusion and metabolism tomograms was measured (*26*).

Segmental myocardial perfusion was labeled as normal (>85% of peak activity), moderately reduced (50 to 85%), or severely reduced (<50%). The ^{18}F-FDG uptake was then normalized to the highest ^{18}F-FDG value of any segment with >85% perfusion uptake, and a 10% decremental, color-coded strata of the normalized myocardial metabolism was created (Figure 1C&1D).

Segments with concordant severely reduced perfusion and metabolism (<50% of peak perfusion and glucose metabolism) were considered 'severe defects' suggesting transmural scar, while reduction of both perfusion and glucose metabolism to 50-70% was labeled as 'moderate defect' consistent with non-transmural scar (*27,28*). Hibernating areas were defined as segments with ^{18}F-FDG uptake that is at least 10% higher than corresponding segmental perfusion (*20*).

Three pre-defined metabolic map characteristics were identified on each ^{18}F-FDG reconstruction before registration:

(i) Metabolic channels were defined as continuous corridors of abnormal metabolism (≤70%) that traversed an area with an even less preserved metabolic activity (≥10% lower than the metabolic channel activity) (Figure 2 & supplemental figure 1)

(ii) Rapid transition areas (RTA) were defined as areas that demonstrated a ≥ 50% increase in PET tracer uptake over the ≤15mm distance in any direction (Figure 3 & supplemental figure 2).

(iii) The metabolic voltage mismatch area (MVM) was defined as an area severe PET defect of ^{18}F-FDG <50%, while the corresponding co-registered LV voltage maps show a preserved bipolar voltage of >1.5mV that accounted for ≥20% of the total LV EAM surface area (Figure 4 & supplemental figure 3).

DICOM3 formatting was applied to Amira output files to allow recognition by the proprietary CartoMERGE software (Biosense Webster, Diamond Bar, USA) and converted to CARTO-3 readable mesh files. The 3D shells were transferred and co-registered to high-density voltage maps using multiple matching landmark pairs (superior/inferior RV septal insertion, mitral valve, apex) using the CartoMERGE Image Processing tool.

VT Ablation

Ablation procedures were performed with a 3.5-mm open irrigated-tip catheter (Thermocool/ Smart touch, Biosense, Diamond Barr, USA). Targeted VT was any clinical VT documented by 12-lead electrocardiograms or presumed clinical VT defined by matching cycle length, far-field morphology, and local electrogram-to-far-field electrogram relationship from ICD recordings.

Radio-frequency (RF) ablation was performed orthogonally to the defined channel using single, overlapping RF lesions (40-50W, the 60s each). After the ablation, programmed

electric stimulation with up to triple extra stimuli and the shortest coupling interval of 200ms from at least 2 RV/LV sites was repeated. Successful ablation of the clinical VT was defined as the inability to re-induce the targeted VT.

Statistical Analysis

All statistical analyses were performed with SPSS 16.0 (SPSS Inc., Chicago, IL, USA). Continuous variables were expressed as mean ± SD and were compared using the Student t-test (normally distributed) or the Mann-Whitney U test (non-normally distributed). For paired variables, the paired t-test or the Wilcoxon signed-rank test were used, respectively. Differences were considered significant at $p < 0.05$.

RESULTS

Patient population

Patient characteristics are shown in Table 1.

All 56 patients had ischemic cardiomyopathy, with ejection fraction (EF) = 29±12%. Most of the patients were males 46/10, with an average age of 63±11 years. All patients had a history of prior myocardial infarction (MI) based on history, Electrocardiography (ECG), and/or cardiac imaging. Ischemic etiology was confirmed by previous coronary intervention with either bypass graft(CABG) (n=20) or prior coronary stenting (n=36). (*29*)

Comparison of Voltage Map with 3D Metabolic Reconstructions

In all patients, 3D PET reconstructions were successfully created and registered. The average reconstruction/registration time was 25±12min. Patients had an average of 1.2±0.4 PET abnormal areas with ≤70% ^{18}F-FDG uptake (minimum size 14.5cm^2) and included in all patients a core area of severe PET defects (<50% uptake).

Severe metabolic defects (<50% uptake) measured 63.0±48.4cm², while PET moderate/severe defects (≤70% uptake) accounted for 105.1±67.2cm², representing 23% and 39% of the total LV surface area, respectively.

Total voltage dense scar area <0.5mV was 13.8±33.1cm², and EAM abnormal voltage area (≤1.5mV) measured 56.2±62.6cm², accounting for 5% and 21% of LV surface area. PET <50% and PET ≤70% were significantly larger than EAM <0.5mV and EAM ≤1.5mv (p<0.001), respectively. However, PET <50% and EAM≤1.5mV area were similar in size p=0.139 (Table 2; Supplemental Figure 4).

Severe PET defects <50% overlapped with voltage scar (<0.5mV) and abnormal voltage (≤1.5mV) 86±22% and 82±18%, respectively. PET defects ≤70% overlapped with voltage scar (<0.5mV) in 91±13% and abnormal voltage (≤1.5mV) in 76±33%.

Analysis of all mapping points (n=23,389) showed that bipolar voltage increased incrementally from PET <50% area (n=10,364; 0.47±0.28mV) to PET 50-70% (n=5,243; 1.51±0.86mV; p<0.01) and PET normal areas (n=7782; 3.2±1.3mV; p<0.001; Figure 5).

VT Ablation and Correlation to Metabolic ^{18}F-FDG Maps

Clinical VTs were successfully induced in 91% of cases (n= 50). Average cycle length (CL) for the induced VTs was 343±96ms. The metabolically abnormal area (PET ≤70%) harbored 88% (n=44, 0.91±0.7 3mV) of the VT channel/exit sites. Severe PET defect area <50% harbored 78% of the VT channel/exit sites (n=39; 0.51±0.32mV) with 28% (n=14), 32% (n=16) and 18% (n=9) localized to areas with ^{18}F-FDG uptake <30%, 30-40% and 40-50%, respectively. Ten percent (n=5; (0.96±0.87mV) of VT channel/exit sites localized to PET 50-70% and 12% of VT channel/exit sites (n=6; 1.31±0.45mV) were in areas with preserved PET activity (>70%) with

average distance of 6.5±3.9 and 13.6±4.5mm from PET≤70% and <50% border , respectively. (Table 3; Supplemental Figure 5).

Hibernation

Hibernation was found in 4 patients (89.2±22.3 cm^2), representing 15.7±10.3% of the LV. Bipolar voltage of hibernating area (n= 1,655 points) was 2.3±1.6 mV, significantly higher than PET<50%, (p= 0.001). Clinical VTs (n=4; CL=259±38ms) were inducible in 3 of the four patients. One VT channel/exit site (25%) localized to the hibernating myocardium (1.2mV; CL=343 ms). The other 3 VT channel/exit sites (75%) localized to PET <50% (0.4±0.2mV). Patients were either poor surgical candidates (n=3) or the hibernating area was deemed too small for revascularization benefit (n=1).

Metabolic Scar Characterization

Metabolic channels: Metabolic channels (n=26) were found in 25 patients (45%;1.1±0.3 channels per patient). The anonymized datasets were independently assessed by an independent blinded reader (SS) with > 20 years of experience in VT ablation to assess the reproducibility of the metabolic channel delineation. All channels (n=26) were identified in the same anatomic locations (100% reproducibility).

The average length/width of the channels were 17.6±12.5mm and 10.3±4.2mm, respectively. 77% (n=20) of the channels demonstrated <50% PET uptake; of those 60 % (n=12) showed PET 30-40% and 40% (n=8) showed PET 40-50% uptake. 23% of the metabolic channels (n=6) showed PET activity 50-70%; of those 33% (n=2) and 67% (n=4) demonstrated PET activity 50-60% and 60-70%, respectively. Channel orientation was more commonly base-to- apex (86%) vs lateral-to -septal 14% (p=0.01).

Thirty-one percent (n=8) of the metabolic channels harbored VT channel/exit sites. All channels that harbored the VT channel /exit sites demonstrated a PET activity of <50%. 63% (n=5) localized to PET 40-50% and 37% (n=3) localized to PET 30-40 % uptake, respectively. Metabolic channels without co-localized VT channel/exit sites (69%; n=18) were at a distance of 12.3±6.4mm from the VT channel/exit sites (Figure 2 & supplemental figure 1).

Rapid Transition Area (RTA): A total of 35 RTAs was found in 33 patients (59%; 1.1±0.2 RTA per patient). RTAs were always localized at metabolic scar/preserved metabolism transition points and were more likely to encompass only a part 81% (n=26) vs. the whole metabolic scar circumference 19% (n=6; p=0.01). The average RTA width/length was 11.8±1.9mm and 53.5±20.4mm, respectively. Ninety percent of RTAs (n=32) demonstrated areas with uptake ranging from <30% up to ≥70% uptake, while 10% (n=3) encompassed areas with ^{18}F-FDG ≥30%up to ≥80% uptake.

RTAs were spatially associated with the VT channel/exits sites. 15% (n=5) of the RTA harbored the VT channel /exit sites, while the rest of the RTA (n=30) was found near (12.8±8.5mm) to the closest VT channel/exit site (Figure 3& supplemental figure 2).

Metabolic-Voltage Mismatches (MVM): Metabolic-Voltage mismatches were detected in 21% (n=12) of patients. The average MVM area accounted for 27±6 % of the LV surface. In patients with MVM, this area (MVM) harbored the VT channel/exit sites in 41% (n=5). The rest of the MVMs (n=7) not harboring the VT channel/exit sites were 14.5±7.8mm from the nearest VT channel/exit site (Figure 4 & supplemental figure 3).

DISCUSSION

The main findings of this study are that functional imaging using decremental color-coded ^{18}F-FDG -PET strata maps can a) detect areas of abnormal myocardial metabolism that harbor ~90% of VT channel/exit sites, b) identify decreased bipolar voltage regions and c) provide a detailed map of regional metabolic remodeling enabling detection of molecular intra-VT substrate heterogeneities/characteristics and possible novel VT ablation targets.

^{18}F-FDG PET is an established gold standard for imaging and differentiating viable from scarred myocardium. ^{18}F-FDG is taken up into the myocardial cells analogously with the serum glucose without further metabolism after phosphorylation, allowing molecular imaging of myocardial cells' metabolic characteristics. Under normal conditions, free fatty acids are the preferred and highly effective cellular pathway for adenosine triphosphate (ATP) production. Ischemia impairs this mitochondrial pathway and shifts it to cytosolic, less-efficient glycolysis-based ATP generation. Under glucose loaded condition, plasma insulin levels increase, and tissue lipolysis is inhibited, resulting in reduced fatty acid delivery to the myocardium and preferred glucose utilization in all viable myocardial cells, regardless of whether they are hypo-perfused or ischemic. Regions with scarred myocardium will have severely decreased or no glucose utilization. Both processes can occur in parallel and with regional heterogeneity within the VT substrate and reflect the molecular and cellular post-ischemic myocardial remodeling and adaption that can be imaged using ^{18}F-FDG (*23*).

Several studies have shown that ^{18}F-FDG has the highest sensitivity in detecting viable myocardium. The cut-off threshold for myocardial viability was different among those studies, but most agreed that segments required uptake ≥ 50% or ≥ 70% to be viable (*27,28*).

Scar Delineation and Scar Size Comparison

Delineation of the myocardial scar using ^{18}F-FDG -PET was able to guide assessing areas with abnormal bipolar voltage. In this study, the ^{18}F-FDG scar was able to predict abnormal bipolar voltage with voltage improving along with the three pre-defined PET categories of PET<50% (severe defect), PET 50-70% (moderate defect), and preserved PET uptake (>70%). The PET-cut-off of <50% used for clinical decisions on revascularization correlated better with the EAM abnormal voltage <1.5mV than ≤70% cut-off, suggesting that a significant metabolic remodeling has to occur before the bipolar voltage is decreased (*27,28*).

In the original ^{18}F-FDG -PET/VT feasibility study (*22*) voltage scar of <0.5mV showed 42±7% PET activity, while EAM 0.5-1.5mV demonstrated a 67±15% tracer uptake with a good PET/EAM scar correlation ($r=0.89$, $p<0.05$). By extension, Tian (*11*) reported a segmental match of 83.7-94.4% between PET and EAM scars. A ROC-based analysis suggested a PET uptake of 46% identified the best abnormal voltage, which is similar to the 50% PET uptake correlated with a voltage of <1.5mV in this study. Furthermore, Fahmy (*17*) identified a bipolar voltage of 0.9mV to best match the PET <50% cut-off with <0.5mV, underestimating PET scar burden. Our finding of a significant increase of PET activity with bipolar voltage is in line with Kettering (*18*), who showed that EAM <0.5mV, 0.5-1mV, and 1-1.5mV correlated with PET activity of 43%, 49.5%, and 60.1%, respectively. The parallel increase of ^{18}F-FDG -PET tracer/voltage and overlap of 86% and 82% between PET<50% and EAM<0.5 and ≤1.5mV, respectively, found in this study, confirms that ^{18}F-FDG -PET uptake can reliably predict low voltage areas in ischemic patients.

All successful ablation sites were located within the PET moderate/severe scar ≤70% (88%) or within 1 cm of its border in metabolically normal tissue (12%). This raises the possibility of either more subtle structural/metabolic changes or may favor functional reentry(*30*).

Metabolic Substrate Characterization of the Post-Infarction VT Substrate

Surviving myocardium within fibrosis areas is a prerequisite of reentrant VT, allowing slow conduction channels to persist (*31,32*). However, recent high-density mapping of post-infarction VT demonstrated that functional block rather than fixed anatomical block defines the VT isthmus's boundaries in up to 80% of cases (*33*).

Functional, post-ischemic remodeling may change the myocardium's electrical conduction properties and potentially contribute to functional block and pro arrhythmicity. To better characterize functional remodeling within the post-ischemic VT substrate, our study assessed three pre-defined metabolic characteristics.

First, 45% of patients were seen as metabolic channels and were oriented more commonly apex-to-base, consistent with reported voltage-based VT channels (*34,35*). Interestingly, the clinical VT channel/exit sites localized in 31% of patients to the metabolic channels. This suggests a potential correlation between functional imaging data -derived channels and clinical VT.

Second, rapid transition areas were pre-defined as regions with >50% metabolic uptake change within 15mm, presumptively identifying a heterogeneous substrate (metabolically preserved adjacent to severe metabolically impaired myocardium). Structural imaging with CMR found that a rapid shift in scar transmurality and heterogeneous LGE ("gray zone") was associated with VT channel location (*7,36,37*). Nearly 60% of patients demonstrated

rapid transition areas, and VT circuits co-localized with RTA in 15% of them. Interestingly, VT channel/exit sites were found either within the RTA or its proximity, raising whether such functional characteristics may correlate with substrate pro-arrhythmicity, such as a functional and fixed block.

Third, metabolic-voltage mismatch areas with severe metabolic defects but preserved bipolar voltage were found in 21% of patients. This demonstrates that the myocardium's severe functional remodeling can occur in a significant number of patients before resulting in measurable bipolar voltage abnormalities. Similar functional discordance has been observed in denervated myocardium with preserved voltage (*12*). Tissue categories with such profound functional heterogeneity may be of arrhythmogenic interest, and MVM areas in this study harbored the VT channel/exit sites in 41%.

STUDY LIMITATIONS

While the largest series to date, the study design was retrospective, and a prospective evaluation will be required for future assessment. PET's spatial resolution is currently in the range of 4–7 mm (*38*). While less than CT, PET technology compares favorably to SPECT (12mm) and is currently the gold standard for functional imaging of the human heart. Registration of the PET imaging datasets and the electroanatomic maps were required to compare the two datasets. Registration errors are inherent in any such process. Still, the use of multiple registration points and careful review of each registration was performed in all cases to minimize any such confounder. The analysis was performed using various pre-defined thresholds and definitions of the PET datasets (such as <50%and ≤70% cut-offs, channels, RTA, and

MVM). It is possible that other cut-offs would have yielded other and yet unknown insights and should be included in future studies.

Further research is needed to compare the functional PET imaging to the LGE-MRI, the gold standard in scar identification.

CONCLUSIONS

3D reconstruction and integration of ^{18}F-FDG functional datasets is feasible and allows the comprehensive assessment of functional remodeling and its heterogeneity in the post-ischemic VT substrate. Detailed 10%-step gradient metabolic maps can reliably predict areas of severe metabolic defects, predict areas of abnormal voltage, and identify ~90% of VT channel/exit sites. Importantly, newly defined metabolic characteristics such as metabolic channels, rapid transition areas, or metabolic-voltage mismatch areas are common and demonstrate heterogeneous intra-substrate remodeling and adaptations within the post-infarct VT substrate.

KEY POINTS:

Question: Is Functional imaging using ^{18}F-FDG - PET prior to VT ablation useful?

Pertinent findings: This is a single-center retrospective study that deals with the drug-refractory VT patients scheduled for VT ablation. We studied the functional imaging characteristics using ^{18}F-FDG - PET. The 3D reconstruction and registration of those ^{18}F-FDG - PET studies were feasible and revealed that the 50 % threshold for scar identification is comparable in size to EAM abnormal voltage area <1.5mV.

The study concluded that new features as metabolic channels, rapid transition area all could provide information about the potential VT substrates

Implications for Patient Care: Using ^{18}F-FDG - PET 3D reconstructions integrated into the Carto maps prior to VT ablations will add valuable information that guides successful substrate identification and ablation.

REFERENCES

1. EM Cronin, FM Bogun, P Maury, et al. HRS/EHRA/APHRS/LAHRS expert consensus statement on catheter ablation of ventricular arrhythmias. *Europace.* 2019;21:1143-1144.

2. Morady F, Harvey M, Kalbfleisch SJ, et al. Radiofrequency catheter ablation of ventricular tachycardia in patients with coronary artery disease. *Circulation.* 1993;87:363-372.

3. Sacher F, Lim HS, Derval N, et al. Substrate Mapping and Ablation for Ventricular Tachycardia: The LAVA approach. *J Cardiovasc Electr.* 2015;4:464-471.

4. Marchlinski FE, Callans DJ, Gottlieb CD, et al. Linear ablation lesions for control of unmappable ventricular tachycardia in patients with ischemic and non-ischemic cardiomyopathy. *Circulation.* 2000;101:1288-1296.

5. Stevenson WG, Wilber DJ, Natale A, et al. Irrigated radiofrequency catheter ablation guided by electroanatomic mapping for recurrent ventricular tachycardia after myocardial infarction: the multicenter thermocool ventricular tachycardia ablation trial. *Circulation* 2008;118:2773-2782.

6. Tian J, Jeudy J, Smith MF, et al. Three-dimensional contrast-enhanced multidetector CT for anatomic, dynamic, and perfusion characterization of abnormal myocardium to guide ventricular tachycardia ablations. *Circ Arrhythm Electrophysiol.* 2010;3:496-504.

7. Dickfeld T, Tian J, Ahmad G, et al. MRI-Guided ventricular tachycardia ablation: integration of late gadolinium-enhanced 3D scar in patients with implantable cardioverter-defibrillators. *Circ Arrhythm Electrophysiol.* 2011;4:172-184.

8. Codreanu A, Odille F, Aliot E, et al. Electroanatomic characterization of post-infarct scars comparison with 3-dimensional myocardial scar reconstruction based on magnetic resonance imaging. *J Am Coll Cardiol.* 2008;52:839-842.

9. Yamashita S, Sacher F, Hooks DA, et al. Myocardial wall thinning predicts transmural substrate in patients with scar-related ventricular tachycardia. *Heart Rhythm.* 2017;14:155-163.

10. Dickfeld T, Lei P, Dilsizian V, et al. Integration of three-dimensional scar maps for ventricular tachycardia ablation with positron emission tomography-computed tomography. *JACC Cardiovasc Imaging.* 2008;1:73-82.

11. Tian J, Smith MF, Chinnadurai P, et al. Clinical application of PET/CT fusion imaging for three-dimensional myocardial scar and left ventricular anatomy during ventricular tachycardia ablation. *J Cardiovasc Electrophysiol.* 2009;20:567-604.

12. Klein T, Abdulghani M, Smith M, et al. Three-Dimensional 123I-Meta-Iodobenzylguanidine Cardiac Innervation Maps to Assess Substrate and Successful Ablation Sites for Ventricular Tachycardia: Feasibility Study for a Novel Paradigm of Innervation Imaging. *Circ Arrhythm Electrophysiol.* 2015;8:583-591.

13. Abdulghani M, Duell J, Smith M, et al. Global and Regional Myocardial Innervation Before and After Ablation of Drug-Refractory Ventricular Tachycardia Assessed with 123I-MIBG. *J Nucl Med.* 2015;56:52S-58S.

14. Mesubi O AG, Jeudy J, Jimenez A, et al. Impact of ICD artifact burden on late gadolinium enhancement cardiac MR imaging in patients undergoing ventricular tachycardia ablation. *Pacing Clin Electrophysiol.* 2014;37:1274-1283.

15. Czernin J, Porenta G, Brunken R, et al. Regional blood flow, oxidative metabolism, and glucose utilization in patients with recent myocardial infarction. *Circulation.* 1993;88:884-895.

16. Tillisch J, Brunken R, Marshall R, et al. Reversibility of cardiac wall-motion abnormalities predicted by positron tomography. *N Engl J Med.* 1986;314:884-888.

17. Fahmy TS, Wazni OM, Jaber WA, et al. Integration of positron emission tomography/computed tomography with electro-anatomical mapping: a novel approach for ablation of scar-related ventricular tachycardia. *Heart Rhythm.* 2008;5:1538-1545.

18. Kettering K, Weig HJ, Reimold M, et al. Catheter ablation of ventricular tachycardias in patients with ischemic cardiomyopathy: validation of voltage mapping criteria for substrate modification by myocardial viability assessment using FDG PET. *Clin Res Cardiol.* 2010;99:753-760.

19. Abdulghani M, Asoglu R, Smith M, et al. Functional molecular imaging characteristics of ischemic and nonischemic scar substrate and successful VT ablation sites using 18F fluorodeoxyglucose (FDG) positron emission tomography. *Circulation.* 2014;130.

20. Hussein AA, Niekoop, M., Dilsizian, V., et al. Hibernating substrate of ventricular tachycardia: a three-dimensional metabolic and electro-anatomic assessment. *J Interv Card Electrophysiol* 2017;48:247.

21. John Duell, Vasken Dilsizian, Mark Smith, et al. Nuclear imaging guidance for ablation of ventricular arrhythmias. *Curr Cardiol Rep.* 2016:18-19.

22. Dickfeld T, Lei P, Dilsizian V, et al. Integration of three-dimensional scar maps for ventricular tachycardia ablation with positron emission tomography-computed tomography. *J Am Coll Cardiol Img.* 2008;1:73-82.

23. Dilsizian V, Stephen L. Bacharach, Rob S. Beanlands, et al. ASNC imaging guidelines/SNMMI procedure standard for positron emission tomography (PET) nuclear cardiology procedures. *J Nucl Cardiol.* 2016;23:1187–1226.

24. Bonow RO, Dilsizian V, Cuocolo A, et al. Identification of viable myocardium in patients with coronary artery disease and left ventricular dysfunction: Comparison of thallium

scintigraphy with reinjection and PET imaging with 18F-fluorodeoxyglucose. *Circulation.* 1991;83:26-37.

25. Dilsizian V, Rocco TP, Freedman NM, et al. Enhanced detection of ischemic but viable myocardium by the reinjection of thallium after stress-redistribution imaging. *N Engl J Med.* 1990;323:141-146.

26. Cerqueira MD, Weissman NJ, Dilsizian V, et al. Standardized myocardial segmentation and nomenclature for tomographic imaging of the heart. *Circulation.* 2002;105:539-542.

27. Schmidt M, Voth E, Schneider CA, et al. F-18-FDG uptake is a reliable predictory of functional recovery of akinetic but viable infarct regions as defined by magnetic resonance imaging before and after revascularization. *Magn Reson Imaging* 2004;22:229-236.

28. Wiggers H, Egeblad H, Nielsen TT, et al. Prediction of reversible myocardial dysfunction by positron emission tomography, low-dose dobutamine echocardiography, resting ECG, and exercise testing. *Cardiology.* 2001;96:32-37.

29. Patel MR, Calhoon JH, Dehmer GJ, et al. ACC/AATS/AHA/ASE/ASNC/SCAI/SCCT/STS 2017 appropriate use criteria for coronary revascularization in patients with stable ischemic heart disease: a report of the American College of Cardiology Appropriate Use Criteria Task Force, American Association for Thoracic Surgery, American Heart Association, American Society of Echocardiography, American Society of Nuclear Cardiology, Society for Cardiovascular

Angiography and Interventions, Society of Cardiovascular Computed Tomography, and Society of Thoracic Surgeons. *J Nucl Cardiol.* 2017;24:1759-1792.

30. Tschabrunn CM RS, Dorman NC, Nezafat R, Josephson ME, Anter E. A swine model of infarct-related reentrant ventricular tachycardia: electroanatomic, magnetic resonance, and histopathological characterization. *Heart rhythm.* 2016;13:262-273.

31. De Bakker J, Van Capelle F, Janse MJ, et al. Slow conduction in the infarcted human heart.'Zigzag'course of activation. *Circulation.* 1993;88:915-926.

32. De Bakker J, Van Capelle F, Janse MJ, et al. Reentry as a cause of ventricular tachycardia in patients with chronic ischemic heart disease: electrophysiologic and anatomic correlation. *Circulation.* 1988;77:589-606.

33. Mark E. Josephson, Elad Anter. Substrate Mapping for Ventricular Tachycardia: Assumptions and Misconceptions. *Jacc clinical electrophysiology.* 2015;1:341-352.

34. Janse MJ, Wit AL. Electrophysiological mechanisms of ventricular arrhythmias resulting from myocardial ischemia and infarction. *Physiological Reviews.* 1989;69:1049-1169.

35. C. de Chillou, D. Lacroix, D. Klug, et al. Isthmus characteristics of reentrant ventricular tachycardia after myocardial infarction. *Circulation.* 2002;105:726-731.

36. Piers Sebastiaan, Qian Tao, Marta de Riva Silva, et al. CMR–Based Identification of Critical Isthmus Sites of Ischemic and Nonischemic Ventricular Tachycardia. *JACC: Cardiovascular imaging.* 2014;7:774-784.

37. Fernández-Armenta J, Berruezo A, Andreu D, et al. Three-dimensional architecture of scar and conducting channels based on high- resolution ce- CMR: insights for ventricular tachycardia ablation. *Circ Arrhythm Electrophysiol.* 2013;6:528-537.

38. Pichler BJ, Wehrl HF, Judenhofer MS. Latest advances in molecular imaging instrumentation. *J Nucl Med.* 2008;49:5S–23S.

Figures:

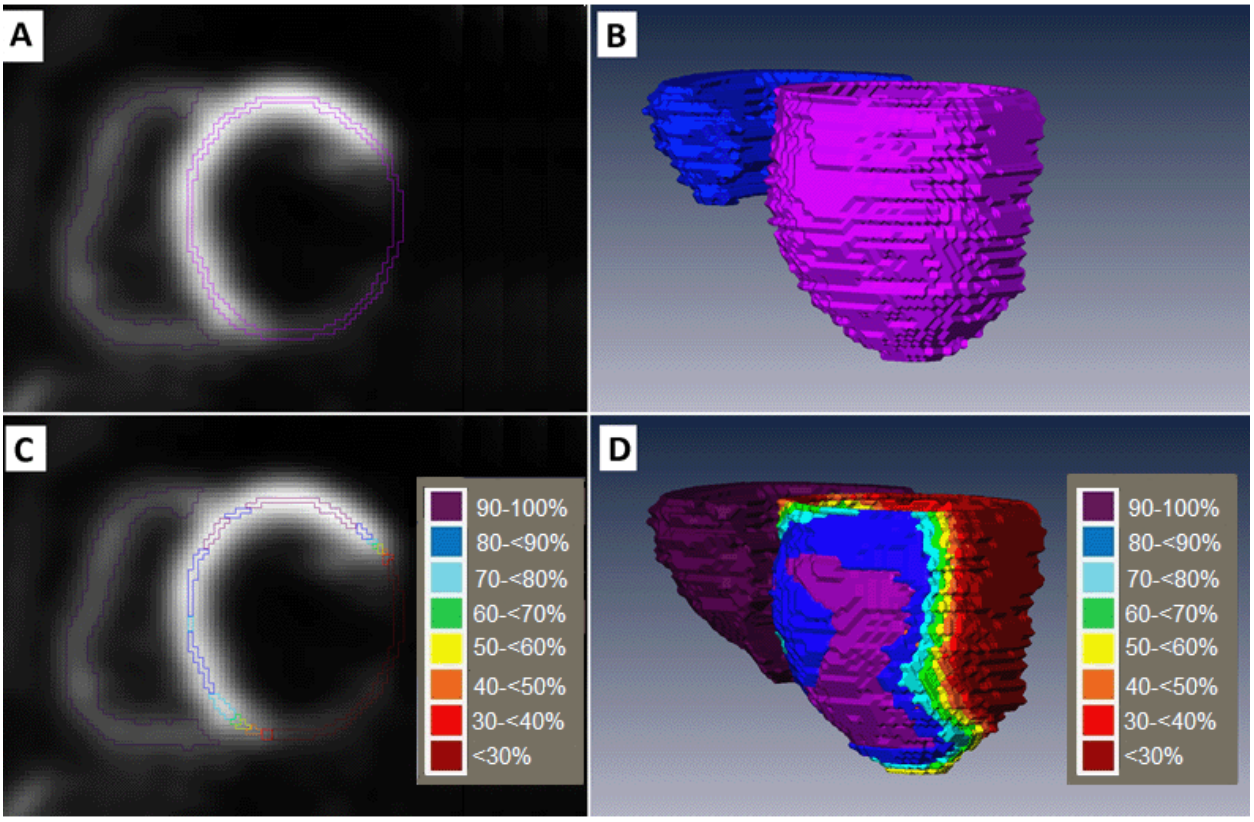

Figure 1**: Workflow of the ^{18}F-FDG Reconstructions. (A)** Raw ^{18}F-FDG -PET DICOM showing left ventricle (LV) with the central region of interest (purple), **(B),** and resulting 3D LV (purple) and RV (blue) reconstruction. **(C)** The same slice, as shown in (A) with the color map according to the value of each segment's ^{18}F-FDG uptake, shows decreased uptake in the inferolateral scar area. **(D)** The generated 3D color PET reconstruction from the SAX slices with the inferolateral scar is based on the ^{18}F-FDG uptake percentage.

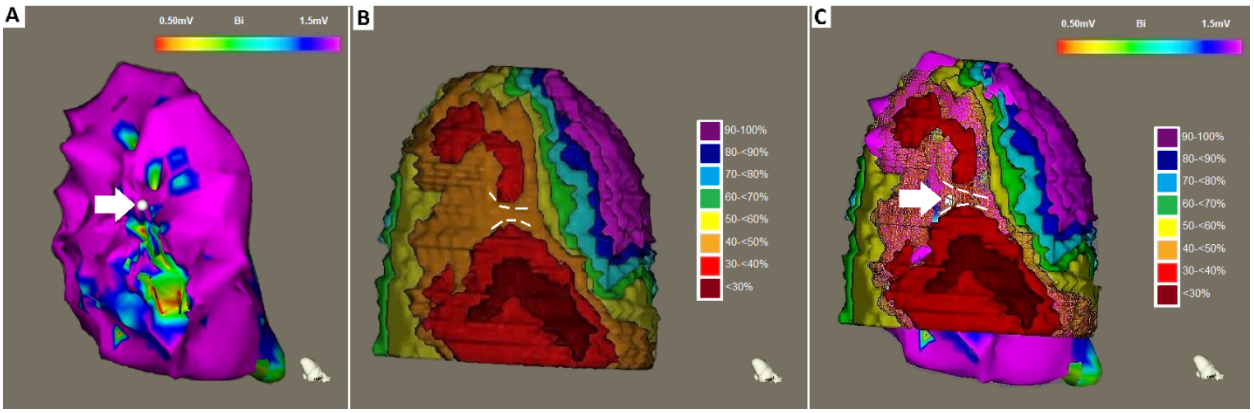

Figure 2: **Metabolic Channel.** (A) EAM shows inferior scar with 0.5-1.5mV settings and VT channel/exit site (white point and arrow). (B) Corresponding PET 3D reconstruction, showing metabolic channel (white dashed lines). (C) Co-registration of EAM and PET 3D reconstruction showing the VT exit /channel (arrow) within the metabolic channel (white dashed lines). Additional example in supplemental material.

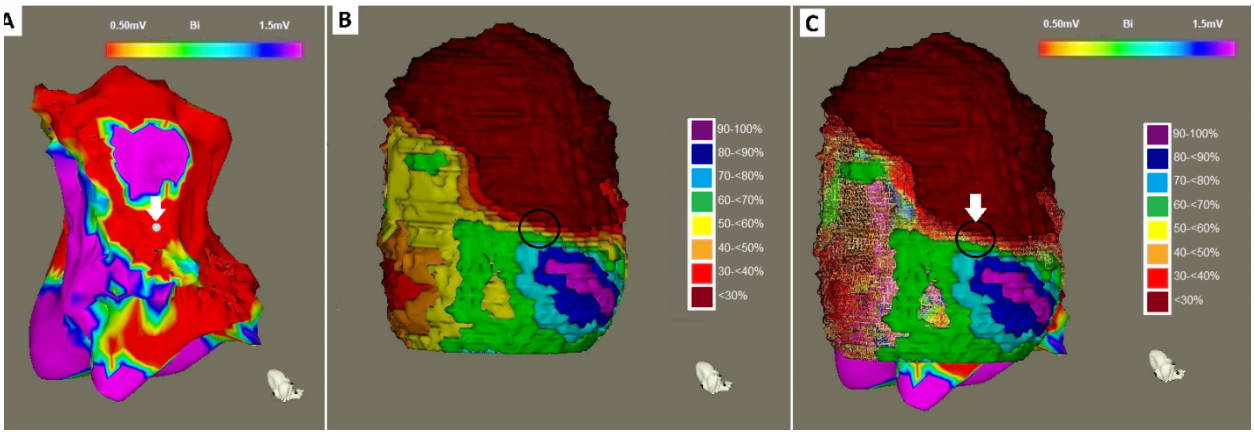

Figure 3: **Rapid Transition Area (RTA).** (A) EAM shows apical &inferior scars with 0.5-1.5mV settings and VT channel /exit site (white point and arrow). (B) PET 3D reconstruction demonstrating RTA (black circle, change of ≥50% uptake/15mm {red to blue color shift}). (C) Co-registration shows the VT exit/ channel within RTA; the white arrow points to the VT channel/exit site within RTA (black circle). Additional example in supplemental material.

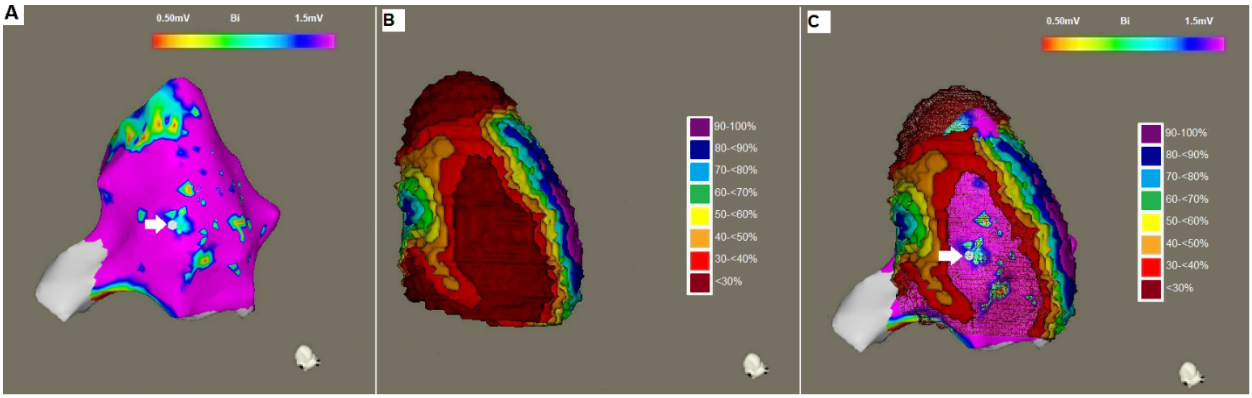

Figure 4: **Metabolic-Voltage Mismatch (MVM).** (A) EAM shows apical &inferior scars with 0.5-1.5mV settings and VT channel /exit site (white point and arrow). (B) PET 3D reconstruction demonstrating larger PET severe defect<50% uptake (red area=MVM). (C) Co-registration of 3D PET reconstruction and EAM demonstrate the VT exit /channel within MVM (white arrow). Additional example in supplemental material.

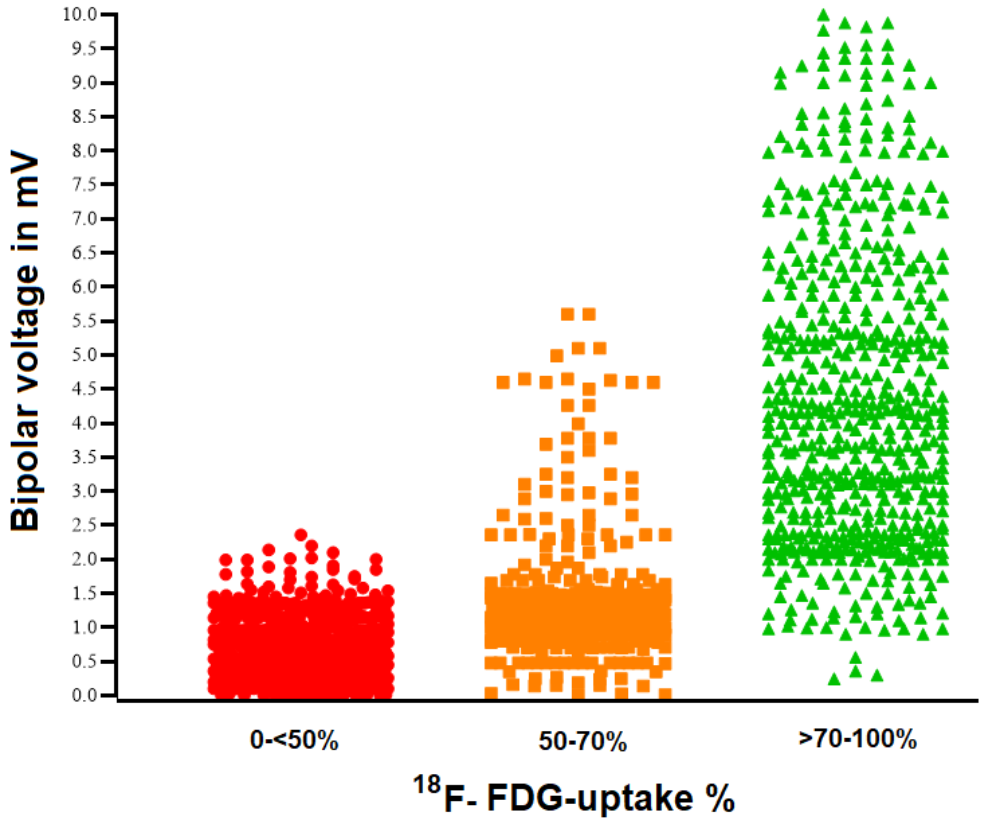

Figure 5: **Bipolar voltage of different PET thresholds.** The average bipolar voltage of severe PET defect <50%, moderate defect 50-70%, and PET normal areas are shown on the scatter plot. There is a stepwise increase in the bipolar voltage with each step of the ^{18}F-FDG PET uptake.

TABLES

Patient criteria	
Age at time of ablation	63±11 years
Gender Male	 46 (82%)
Ejection fraction (EF) %	29±12 %
Ischemic Previous myocardial infarction (History, ECG, or cardiac imaging) Bypass graft Coronary stenting	 56 (100%) 20 (36%) 36 (64%)
Heart failure NYHA (II-III)	25 (45%)
Diabetes	17 (30%)
Hypertension	30 (54%)
ICD at time of ablation	35 (63%)
^{18}F-FDG - PET scar <50% uptake.	-Inferior (infero-lateral and infero-septal scar n= 38(70%) -Anterior scar (antero-septal and antero-lateral n=12 (23%) -Apical scar n=3 (3.5%) -Anterior and inferior scar n=3 (3.5%)
EAM scar <0.5mv	n= 53 (97%)
Anti -Arrhythmic drugs	B-blockers n=52 (93%). Amiodarone n=46(82%) Sotalol n=5 (9%)

NYHA New York heart association; ICD, Implantable cardioverter-defibrillator.
Table 1 Patient Characteristics. Data are presented as mean±SD or n (%).

	Area size (cm^2)	Percentages out of the total LV EAM
Total LV EAM	270.2±10.3	
Severe PET defect <50%	63.0±48.4	23%
Moderate/severe PET defect ≤70%	105.1±67.2	39%
EAM voltage scar <0.5mV	13.8±33.1	5%
EAM abnormal Voltage ≤1.5mV	56.2±62.6	21%

Table 2 Imaging Characteristics. Continuous variables are expressed mean±SD or n (%).

		Voltage Map	
		Voltage scar <0.5mV	Abnormal voltage 0.5-1.5mV
^{18}F-FDG -PET Percentage	<30%	5	9
	30 - <40%	6	10
	40 - <50%	1	8
	50-70%	0	5
	>70%	0	6

Table 3: ^{18}F-FDG Uptake of VT Channel/Exit Sites (n=50). Distribution of ^{18}F-FDG uptake percentage and bipolar voltage characteristics of the clinically determined VT channel/exit sites.

Supplemental Material – Figures

Supplemental Figure 1:

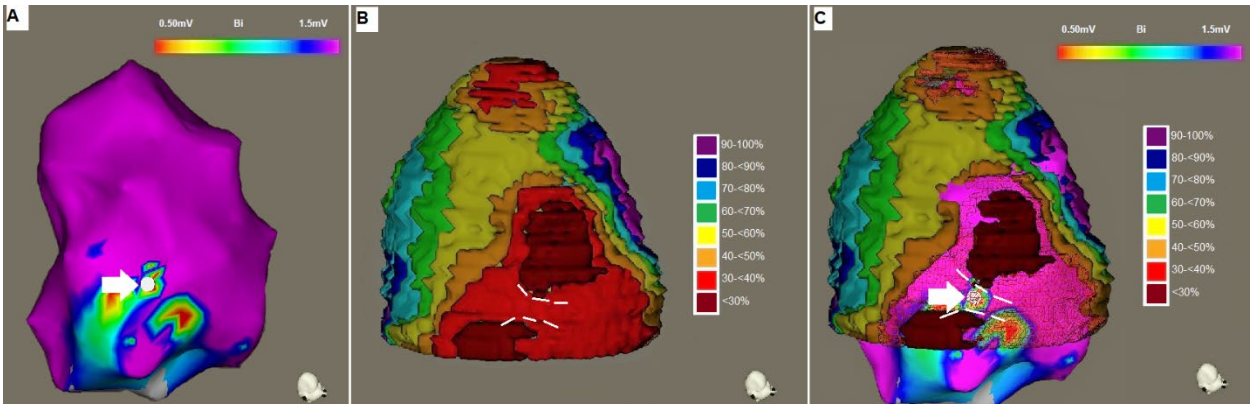

Metabolic Channel (additional example). (A) EAM shows inferior scar with 0.5-1.5mV settings and VT channel/exit site (white point and arrow). (B) Corresponding PET 3D reconstruction, showing metabolic channel (white dashed lines). (C) Co-registration of EAM and PET 3D reconstruction showing the VT exit /channel (arrow) within the metabolic channel (white dashed lines).

Supplemental Figure 2:

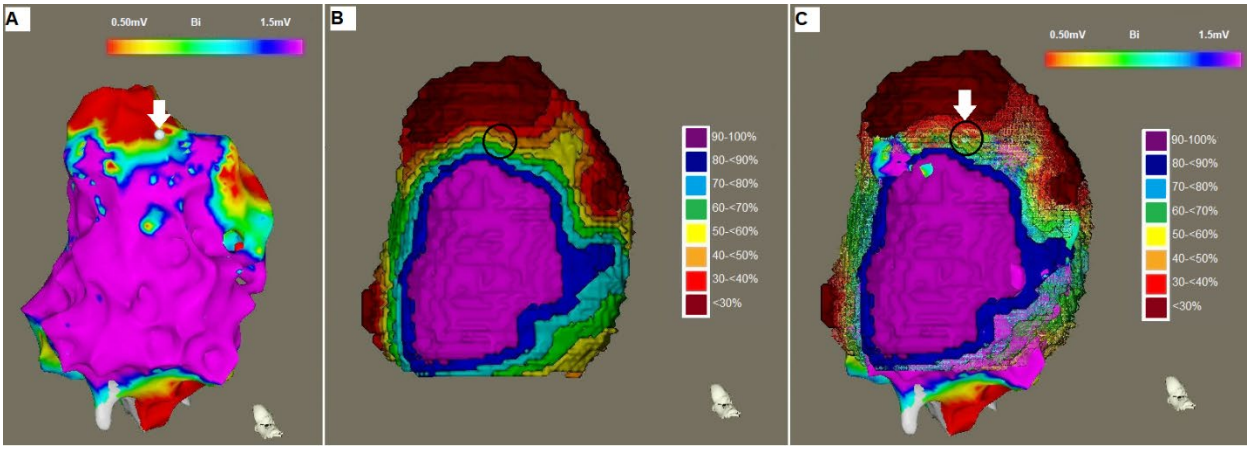

Rapid Transition Area (RTA; additional example). (A) EAM shows apical scar with 0.5-1.5mV settings and VT channel /exit site (white point and arrow). (B) PET 3D reconstruction demonstrating RTA (black circle, change of ≥50% uptake/15mm {red to blue color shift}). (C) Co-registration shows the VT exit/ channel within RTA; the white arrow points to the VT channel/exit site within RTA (black circle).

Supplemental Figure 3:

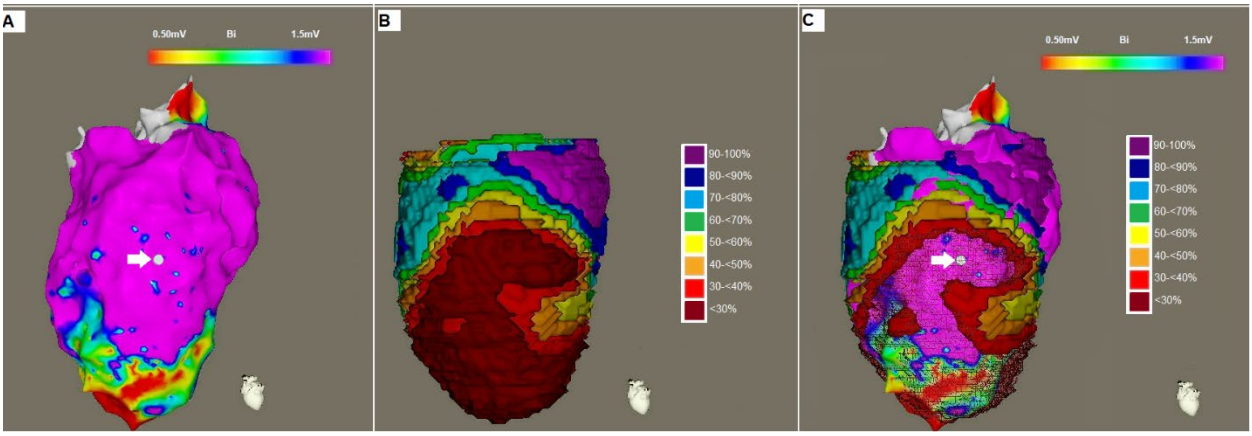

Metabolic-Voltage Mismatch (MVM; additional example). (A) EAM shows apical &inferior scars with 0.5-1.5mV settings and VT channel /exit site (white point and arrow). (B) PET 3D reconstruction demonstrating larger PET severe defect<50% uptake (red area=MVM). (C) Co-registration of 3D PET reconstruction and EAM demonstrate the VT exit /channel within MVM (white arrow).

Supplemental Figure 4:

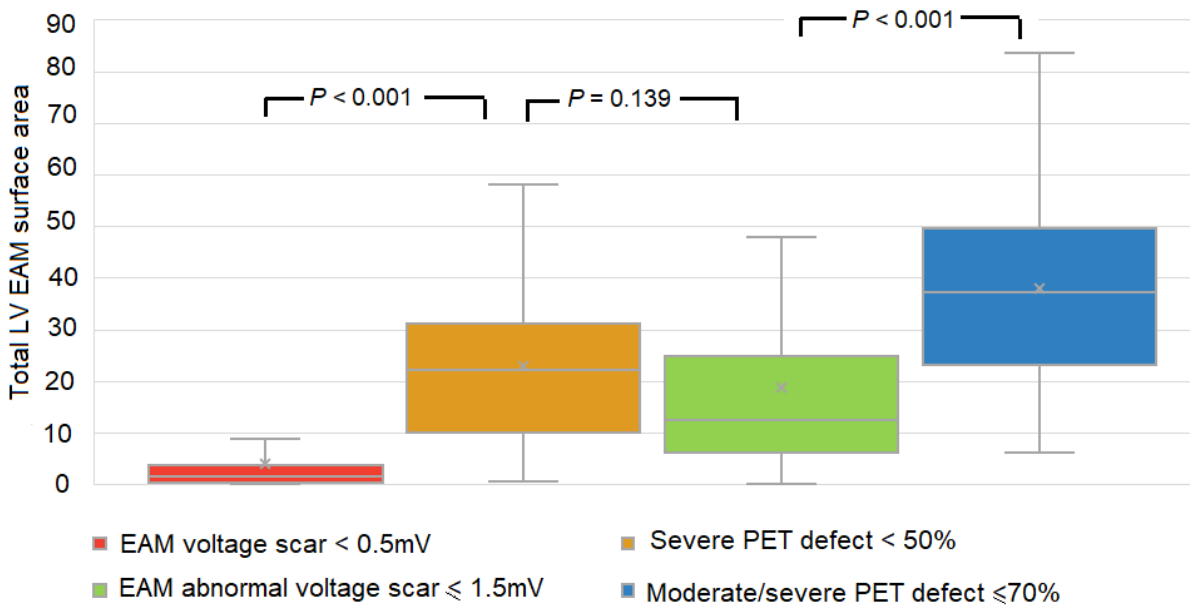

Graphical representation Comparing the size of abnormal VT Substrate areas out of total LV surface [mean± SD].

Supplemental Figure 5:

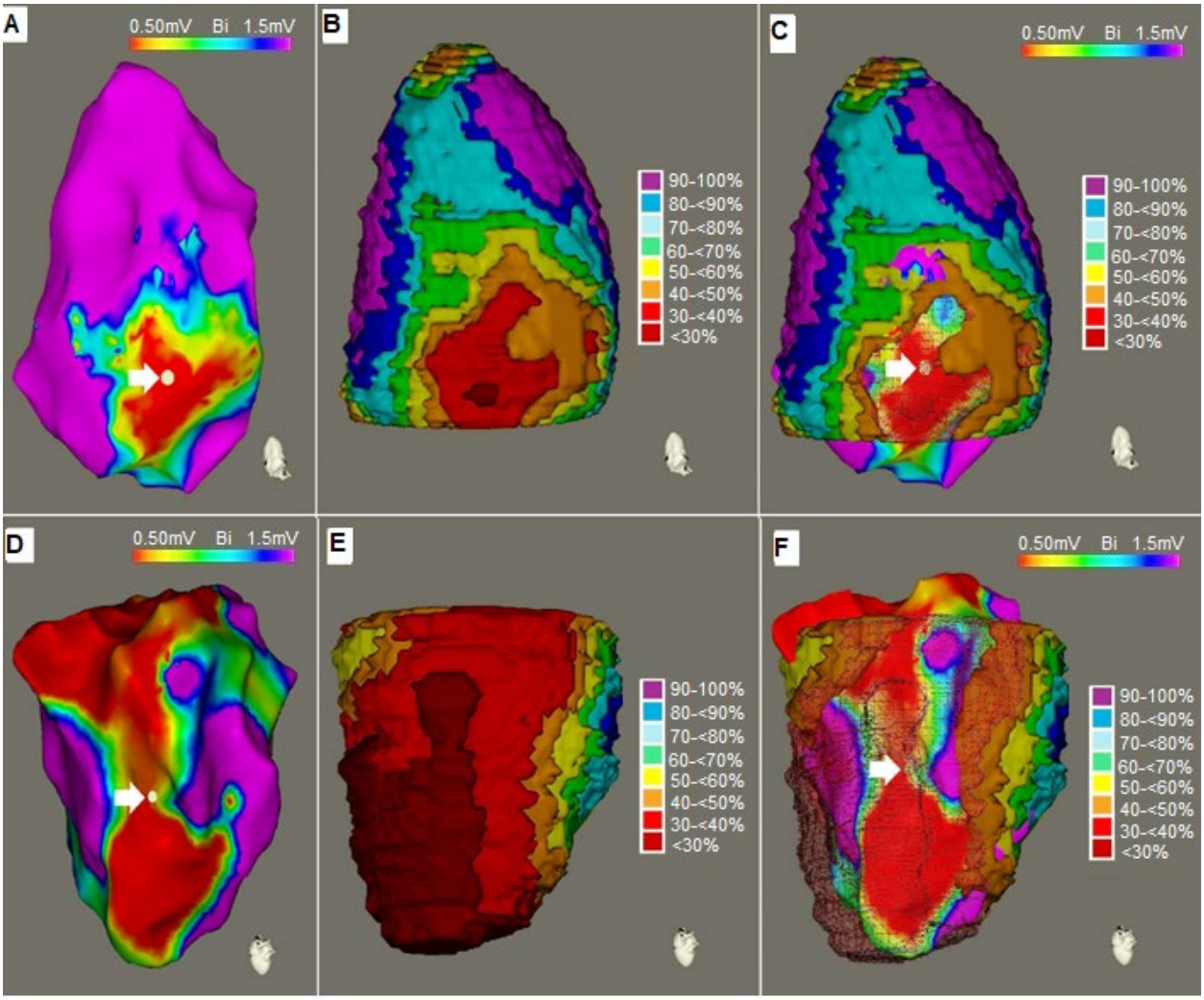

Correlation of Abnormal Voltage and ^{18}F-FDG Uptake. (A & D): EAMs showing inferior scar, threshold adjusted 0.5-1.5mV, the white points represent the VT exit/channel. **(B & E)** show the corresponding ^{18}-FDG 3D reconstructions; both show good correlations of scar location and size to the EAM. **(C & F)** show the registered EAM and ^{18}-FDG reconstruction with the VT exit site/channel (white arrow**)** seen within the co-registered scar areas.